Journal of Inflammation Research

Dovepress
Taylor & Francis Group

Open Access Full Text Article

ORIGINAL RESEARCH

Investigating the Underlying Mechanisms of Ma-Xing-Shi-Gan-Tang on Asthma via Metabolomics and Network Pharmacology

Yang Yu[1], Songquan Wu[1], Tiantian Sun[2], Zhiyi Zhou[1], Linyan Xu[1], Dinghan Peng[1], Xin Fu[1]

[1]College of Medicine, Lishui University, Lishui, 323000, People's Republic of China; [2]College of Pharmacy, Heilongjiang University of Traditional Chinese Medicine, Harbin, 150040, People's Republic of China

Correspondence: Xin Fu, Email fu19511317872@sina.com

Objective: Ma-xing-shi-gan-tan (MXSGT) was first published in "Shang-han-lun". It functions as a heat-clearing agent, lung-clearing formula, and asthma reliever. This study aims to evaluate the therapeutic effect of MXSGT on asthma and elucidate its underlying mechanisms.

Methods: Key components of MXSGT were identified using ultra-performance liquid chromatography-tandem mass spectrometry (UPLC-MS). A rat model of asthma induced by ovalbumin (OVA) was employed to assess MXSGT efficacy. The fundamental mechanisms of MXSGT in asthma treatment were investigated through metabolomic analysis, network pharmacology, and molecular docking.

Results: MXSGT treatment demonstrated significant protective effects in OVA-induced asthmatic rats, evidenced by its suppression of inflammatory mediators including nuclear factor kappa B complex p65 (NF-κBp65), p38 mitogen-activated protein kinase (p38-MAPK), and transforming growth factor-β1 (TGF-β1). Metabolomic analysis revealed 9 MXSGT blood components and 12 differential metabolites associated with MXSGT treatment. Further analysis indicated that MXSGT's therapeutic benefit in asthma involves modulation of metabolic pathways such as the citric acid cycle (TCA cycle), alanine and aspartate metabolism, tyrosine metabolism, among others. Succinic acid was identified as the metabolite most prominently involved in these pathways. Additionally, network pharmacology identified TNF as a key target linking blood components and differential metabolites, mediating anti-asthma effects through MAPK and NF-κB signaling pathways.

Conclusion: Our findings demonstrate that MXSGT exerts anti-inflammatory effects in asthma treatment by inhibiting MAPK and NF-κB signaling pathways and regulating host metabolites and metabolic pathways. These insights provide novel perspectives on MXSGT's role in asthma management.

Keywords: Ma-Xing-Shi-Gan-Tang, asthma, metabolomics, network pharmacology, signaling pathway

Introduction

Asthma is a common allergic disease affecting individuals across all age groups globally, imposing a substantial burden on global healthcare resources.[1] Typically characterized as a heterogeneous clinical syndrome, asthma presents with reversible airflow limitation, bronchial hyperresponsiveness, chronic airway inflammation, and hallmark symptoms including wheezing, dyspnea, chest tightness, and cough.[2] These shared clinical features define recognizable asthma phenotypes. However, contemporary research has revealed significant underlying heterogeneity within this common phenotype, arising from distinct intrinsic biological mechanisms or endotypes.[3] These endotypes represent unique pathogenic processes driven by specific molecular pathways (eg, Th2-high, Th2-low, or neutrophilic inflammation), cellular populations, genetic, and environmental factors.[4,5] Notably, the OVA-induced rat asthma model recapitulates a specific asthma subtype dominated by Th2-type inflammatory responses.[6]

Ma-xing-shi-gan-tang (MXSGT) is a famous prescription recorded in the "Shang-han-lun". MXSGT contains four traditional Chinese herbs, ephedra, licorice, almond, and mineral gypsum.[7] MXSGT has significant therapeutic effects on cold, asthma, and upper respiratory tract infections.[8] Therefore, it is widely used in clinical practice with over 2000

Received: 3 March 2025
Accepted: 7 August 2025
Published: 18 August 2025

years.[9] Modern pharmacological studies have shown that the three traditional Chinese medicine (TCM) in MXSGT formula, ephedra, almond, licorice, and mineral gypsum, all have therapeutic effects on asthma. The active ingredient ephedrine, pseudoephedrine and methylephedrine in ephedra,[10] the active ingredient amygdalin in almond and the active ingredient licoriceglycyrrhizic acid and glycyrrhetinic acid in licorice have been proven to have therapeutic effects on asthma.[11,12] However, the specific molecular mechanism of MXSGT in treating asthma is not clear to us.

Metabolomics approaches focus on quantitative and qualitative analyses of small molecular metabolites from normal or abnormal cells induced by genetic modification or pathophysiological stimulation. To investigate the pathogenic mechanisms of asthma, metabolomics provides a new integrated systems approach, especially for endogenous compounds and their dynamic changes.[13] Metabolomics combines with advanced instruments and appropriate data processing, which may provide supports to explain the mechanism of MXSGT. Metabolomics is a comprehensive approach for the study of metabolites in biological sample. Many scientists have used metabolomics technology to research TCM.[14,15] Network pharmacology is a new interdisciplinary subject. It is based on the theory of systems biology, also integrated bioinformatics and network analysis methods. It is used to study the mechanism of drugs and design multi-target drugs at the system level.[16,17] Metabolomics, which based on Ultra performance liquid chromatography (UPLC) and mass spectrometry (MS) can identify biomarkers and detect changes at molecular compounds in biological systems.[18] Network pharmacology can be used to analyze relationships between drugs, targets, metabolic pathways, and diseases by constructing network models.[19] Therefore, the combination of metabonomics and network pharmacology is helpful to the mechanism of MXSGT in asthma's treating. The application of metabolomics and network pharmacology method to investigate MXSGT in treating asthma have yet to be reported. So we examined the therapeutic mechanism of MXSGT in this work.

Materials and Methods

Chemicals and Reagents

The herbs *Ephedra sinica Stapf* (MA-HUANG; batch number 1410030M; Check no. 2014-CP-10038) (Inner Mongolia province), *Prunus mandshurica* (Maxim). *Koehne* (XING-REN; batch number 1401074ch; Check no. 2014-CP-01106) (Hebei province), *Gypsum Fibrosum* (SHI-GAO; batch number 1407025S; 2014-CP-07044) (Hebei province), and *Glycyrrhiza uralensis Fisch*. (GAN-CAO; batch number 1503036M; 2014-CP-03027) (Inner Mongolia province) were purchased from Harbin Pharmaceutical Group Co., Ltd. (HPGC) (Heilongjiang province, China in 2014). The Chinese medicine slices were identified by Lianjie Su of Heilongjiang University of Chinese Medicine. HPLC-grade acetonitrile (Fisher Scientific, USA; Cat. No. 148407), HPLC-grade methanol (Fisher, USA), and formic acid (Sigma Chemical Co., USA; Cat. No. 110301) were used. OVA (Sigma A-5253) and ultra-pure water (Watson's Food & Beverage Co., Ltd., China) were purchased.

Preparation of MXSGT Samples

According to the instruction recorded in "Shang-han-lun", MXSGT was prepared in the following procedures. Firstly, *Ephedra sinica Stapf*. (9g) immersed in 700 mL deionized water and then decocted to boiling for 30 min until the volume of water reduced to 500 mL and then get rid of the foam. Secondly, add *Prunus mandshurica (Maxim). Koehne* (9g), *Gypsum Fibrosum* (18g), *Glycyrrhizauralensis Fisch* (6g) Toitand.

Then decocted to boiling for 1h until the volume of water reduced to about 200mL. The process was repeated 3 times before combining three filtrates. Supernatant of extraction solution was filtered via 6 layers gauze and made to concentration of 1g crude drug per milliliter, and the decoction was transformed into the freeze-dried.

Experiments on Animal

Animals

Twenty-four healthy eight-week-old male Sprague-Dawley rats (200 ± 20 g) were obtained from the experimental animal center of Heilongjiang University of Chinese Medicine. The experimental protocols were approved by the Animal Care and Use Committee of Heilongjiang University of Chinese Medicine (HUCM-201608212) and conducted in strict

accordance with the Chinese National Standard "Guidelines for Ethical Review of Laboratory Animal Welfare" (GB/T 35892–2018). All rats were raised in an environment with humidity (50 ± 5%) and constant temperature (23 ± 2°C) and were exposed to light for 12 h each day. Prior to treatment, all the animals were permitted to adapt their metabolism for one week. The rats were fed with standard laboratory's chow and water was provided ad libitum.

Animal Care and Diet

All the rats were randomly divided into three groups of eight rats each: control group, model group, and treatment group (MXSGT). On the 1st and 8th days, rats from the model group and treatment group were injected subcutaneously with 1 mL of a solution containing 1% OVA and 100 mg $Al(OH)_3$ daily to induce sensitization. Instead, rats in the control group were injected subcutaneously with 1 mL of saline daily. From days 16–22, rats from the model and treatment group were challenged with 1%OVA aerosol for 30 minutes. Rats from the model group were challenged with saline aerosol. From days 18–21, rats in the treatment group were intragastrically administered MXSGT (dissolved in saline) at a dose of 1 mL/100 g once daily. Rats from the control group and the model group were given the same volume of normal saline. The dosage of MXSGT is calculated as the equivalent dose based on the ratio of body surface area between humans and animals, and the calculated result is 10mg/kg.

Sample Collection and Preparation

The blood samples were collected from the hepatic portal vein at 30 min after administration and all animals were fasted on the 22th day and then sacrificed. Plasma was separated from whole blood via centrifugation at 13000 rpm at 4°C for 10 min, then the plasma was analyzed by using the UPLC-MS system with an injection volume of 5μL.

HE Staining Detection of Relevant Pathological Changes

Extract lung tissue from 10% paraformaldehyde, dehydrate it with gradient ethanol and xylene, and wrap it in paraffin Burial, slice continuously with a slicer (6 μm thickness), and prepare paraffin sections. Xylene, gradient ethanol dewaxing, hematoxylin and eosin staining, gradient ethyl Dehydration with alcohol and xylene, and sealing with neutral gum. Observe pathological structural changes under a microscope at 400x magnification.

Immunohistochemical Detection

Dissolve the paraffin embedded lung tissue slices in water, incubate in 3% H2O2 for 10 minutes, wash with PBS for 2 minutes 3 times, and transfer the slices into citrate buffer (pH 6). Microwave the slices twice every 5 minutes with a 10 minute interval in between. Cool naturally to room temperature. Add primary antibody dropwise, refrigerate overnight at 4 degrees Celsius, wash with PBS for 2 minutes 3 times. Add secondary antibody dropwise, incubate at 37 °C for 30 minutes, wash with PBS for 2 minutes 3 times. DAB color development takes 5–10 minutes. Rinse thoroughly with distilled water. After counterstaining with hematoxylin for 1 minute, the sample was dehydrated and transparent, then sealed with neutral gum and observed under a 400x microscope.

Analysis of Metabolomics

Chromatography

A Waters Acquity Ultra Performance LC system (Waters Corp., Milford, MA, USA) was used to separate metabolites under control of Masslynx (V4.1, Waters Corporation) equipped with an HSS T3 column (2.1 mm × 100 mm, 1.7 μm, UK). The temperature of the column was set at 40°C, and the gradient elution program was operated with 98% solvent A and 2% solvent B. The former was a 0.1% acetonitrile solution of formic acid, and the latter was water with 0.1% formic acid. The column was subjected to elution over a linear gradient of 98–2% A for 0.5 to 9 min, 2–98% A for 2 to 10 min, and 98% A for 1 min, with a flow rate of 0.40 mL/min.

MS

High-definition mass spectrometry was performed on an AB SCIEX Triple TOF 5600 equipped with an electrospray ion (ESI) source for mass spectrometry in both positive and negative ion modes. The data were acquired from m/z 50 to m/z 1200. During the experiment, the Ion Source Gas1 (Gs1) 50L/h, the Ion Source Gas2 (Gs2) 50L/h, the IonSpray Voltage Floating (ISVF) +1.0 KV, the Interface Heater Temperature (IHT) 150°C, the Curtain Gas (CUR) 20L/h, the Declustering

Potential (DP) +40 V, the Collision Energy (CE) +30 V, the Collision Energy Spread (CES) 15 V in positive ion mode; the Gs1 50 L/h, the Gs2 50 L/h, the ISVF −1.0 KV, the IHT 150°C, the CUR 20 L/h, the DP −40 V, the CE −30 V, the Collision Energy Spread (CES) 15 V in negative ion mode.

Data Processing and Multivariate Data Analysis

Progenesis QI 1.0 software was used to process the raw data files for quantitative metabolomics, and then, EZinfo 3.0 software was used to analyze the multivariate data. The available on-line databases, including KEGG, HMDB, TCMSP, PubChem, RCSB PDB, Massbank, Chemspider were utilized to analyze potential biomarkers and Cytoscape 3.10.2 was used to calculate the degree of asthma-target, and then, the Metscape plugin in Cytoscape and MetPA tool were used to analyze the pathways of the biomarkers.

Identification of Biomarkers

The quantification of compounds was conducted with commercial databases by using precise MS/MS fragments. Based on the above protocols, an objective and strict matching analysis was used to the automatic identification system of the Progenesis QI software.

Statistical Analysis

SPSS software (Version 22.0 for windows, IBM, Chicago, IL) was used for the statistical analysis of the ions between the control and model groups. The content of the ions between the two groups was compared to filtering the difference, and the P value of Student's *t*-test was less than 0.05. Using the combined VIP lists of OPLS-DA and the p values of the *t* tests, a series of biomarkers were identified to reflect differences in metabolites.

Network Pharmacology

Target Prediction

Using the TCMSP (https://old.tcmsp-e.com/tcmsp.php), SwissADME (http://www.swissadme.ch/), SwissTarget Predictiondatabases (http://www.swisstargetprediction.ch/), GeneCards (https://www.chemsrc.com/casindex/) and Home-OMIM (https://omim.org/) to predict the active ingredient targets and disease targets. This data is secondary data and does not contain any data which can identify individual. Therefore, ethical approval is exempted. The requirement for informed consent was waived because this study was based on routinely collected claims data.

Construction of a PPI Network Diagram and Screening of the Core Targets

Using the online tool VENNY2.1 (https://bioinfogp.cnb.csic.es/tools/venny/) to intersect the active ingredient targets and treatment targets for asthma and obtain potential treatment targets. After that, importing them into the STRING database (https://www.stringdb.org/) searching the species "Homo sapiens", with the minimum interaction score of "≥0.400". MCC was used to screen out the top 10 core targets based on the relationship between nodes and edges. Then use Cytoscape 3.10.2 to construct a network diagram of interacting targets.

GO Enrichment Analysis and KEGG Pathway Analysis

Exploring potential molecular mechanisms through GO enrichment analysis, including BP, CC, and MF. We also use KEGG pathway analysis to identify biological functions and candidate targets. David database (https://david.ncifcrf.gov/home.jsp) was used to GO enrichment analysis and KEGG pathway analysis on intersecting targets. The results were visualized using Wei Sheng Xin (https://www.bioinformatics.com.cn/).

Target-Based Classification of Drugs

Input key targets into the target-based drug classification in KEGG (https://www.kegg.jp/brite/br08310) and search for relevant signaling pathways related to experimental results.

Molecular Docking

AutoDockTools 1.5.7 and PyMOL were employed for molecular docking and visual analysis. The structure of pseudoephedrine, and glycyrrhetinic acid were obtained from PubChem (https://pubchem.ncbi.nlm.nih.gov/), while the core target TNF

(PDB: 6q01) was retrieved from the PDB database (https://www.rcsb.org/). We chose an adequate docking box to cover the complete protein after de-watering and hydrogenation, and the docking findings were displayed using PyMOL.

Results

Histopathological and Immunohistochemical Analyses

From the histopathological observations, a significant change in the microscopic histology of HE stained lung sections was detected in the OVA-induced asthma rat (model) groups. Specifically, compared with the control rats, these rats showed mucosa thickening, luminal narrowing and marked infiltration of inflammatory cells into perivascular and connective tissues. The HE staining results are shown in Figure 1.

In the control group, the bronchial mucosa epithelium was orderly arranged, the lumen did not shrink, and no inflammatory cell infiltration was observed. In the model group, the bronchiolar mucosa epithelium was disordered, with focal detachment, thickening of the basement membrane, thickening of the bronchial wall, stenosis of the lumen, infiltration of a large number of inflammatory cells, capillary congestion, etc. Hyperemia, edema, and inflammatory cell infiltration persisted in the mucosa of the MXSGT group, but these were significantly reduced compared with the model group. The infiltration of inflammatory cells in the MXSGT group was less than in the model group, and there were a few epithelial cells and inflammatory cells in the lumen; the bronchial lumen was enlarged, the alveolar septum was significantly thinner, the alveolar cavity was enlarged, and the pathological changes were significantly improved.

In immunohistochemical analysis, compared with the control group, the expression of nuclear factor kappa B complex p65 (NF-κBp65) protein in the lung tissue of the model group was increased, and the difference between the two groups was statistically significant ($P < 0.001$). The expression of NF-κBp65 in the lung tissue of the MXSGT group was lower than that in the model group ($P < 0.001$). The expression of p38 mitogen-activated protein kinase (p38-MAPK) protein in rat lung tissue of the model group was increased compared with that in the control group, and the difference between the two groups was statistically significant ($P < 0.001$), and the expression of p38-MAPK in MXSGT-treated lung tissue was lower than that in the model group ($P < 0.001$). Transforming growth factor-β1 (TGF-β1) protein expression in the lung tissues of the model group was increased compared with that of the control group, and the difference between the two groups was statistically significant ($P < 0.001$). The expression of TGF-β1 in MXSGT-treated lung tissue was lower than that in the model group ($P < 0.001$), and the expression of TGF-β1 in MXSGT lung tissue was lower than that in the model group ($P < 0.001$). The results for the expression of NF-κBp65, p38-MAPK and TGF-β1 are shown in Figure 2.

The Main Blood Components in MXSGT

Administered rat serum was analyzed using UPLC-MS, and base peak ion chromatograms were obtained in both positive and negative ion modes. We identified MXSGT blood components (Table 1)) through database comparison.

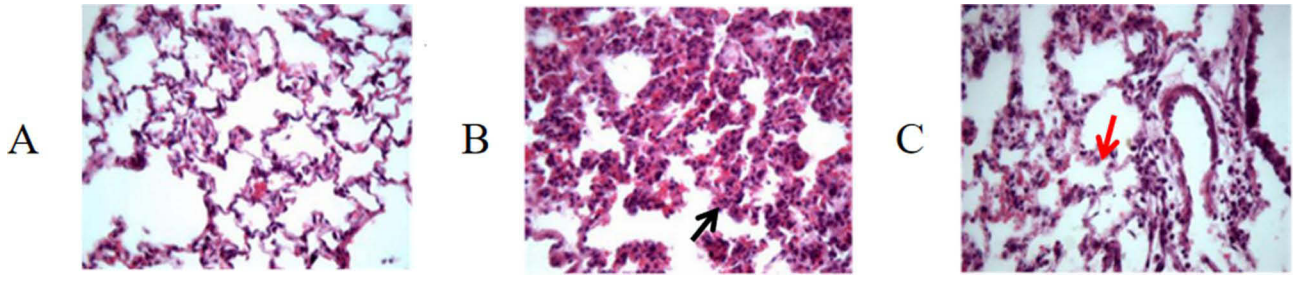

Figure 1 Representative HE staining (400×) of lung sections from control Rat and OVA-induced asthma Rat on 22th day. The black arrow represents the presence of inflammatory cell infiltration and red arrow represents the infiltration of inflammatory cells have been improved, (**A**) Control group; (**B**) Model group; (**C**) Treatment group.

https://doi.org/10.2147/JIR.S515631

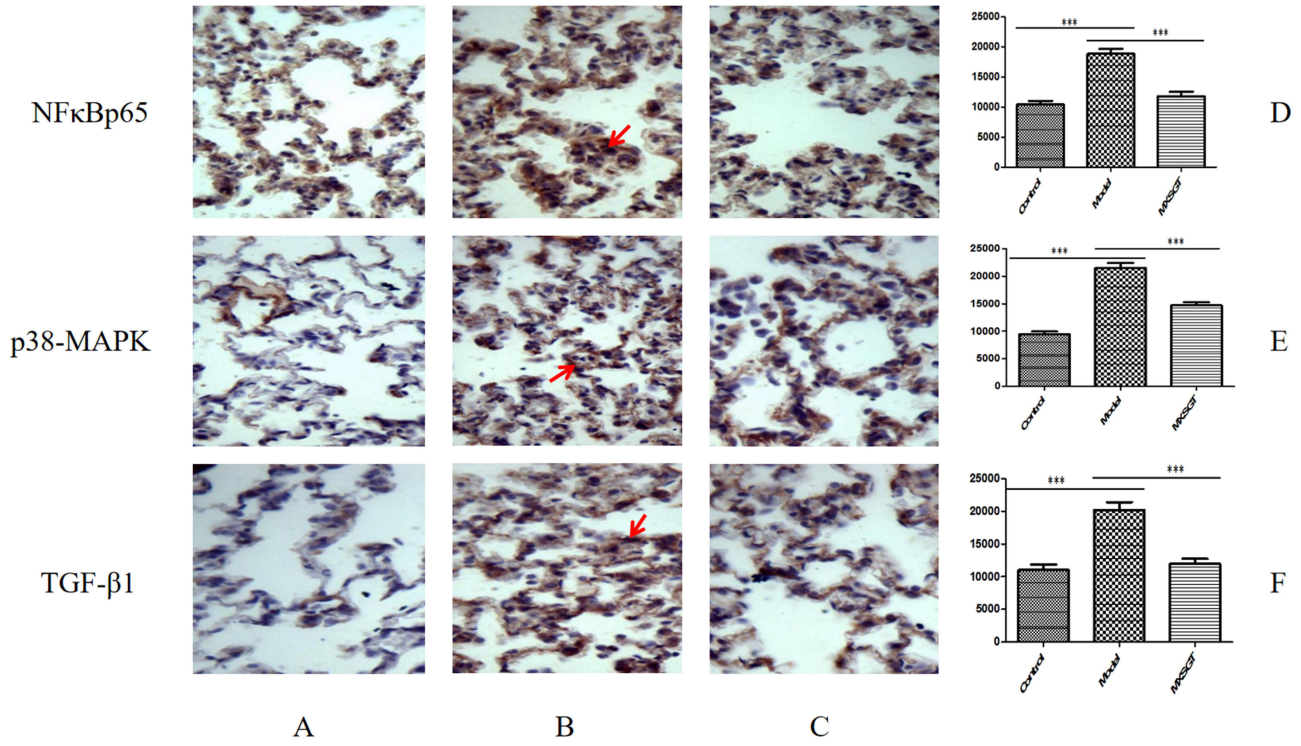

Figure 2 The expression of NFκBp65, p38-MAPK, TGF-β1 in immunohistochemical analysis (magnification 400x, ***P < 0.001). The red arrow represents immunohistochemistry positive cells. (**A**) Control Group; (**B**) Mode Group; (**C**) Treatment Group; (**D**) The expression of NFκBp65; (**E**) The expression of p38-MAPK; (**F**) The expression of TGF-β1 in immunohistochemical analysis.

Effects of MXSGT in OVA-Induced Rats

In both positive and negative ion modes, the control group and the model group were well separated, indicating that asthma affects the blood metabolic spectrum. After MXSGT administration, in the same modes, the control group remained well-separated from the model group, while the MXSGT group clustered closer to the control group, indicating metabolic reversal in the MXSGT group. The S-plot significantly contributed to dataset classification by screening differential variables in positive and negative ion modes (Figure 3).

Table 1 MXSGT Blood Components

No.	Rt (min)	Name	Formula	Ms/Ms	m/z
1	0.72	Gancaonin H	$C_{21}H_{20}O_6$	[M + H]+	421.1
2	0.72	Glabridin	$C_{20}H_{20}O_4$	[M + H]+	325.1
3	1.22	Ephedrine	$C_{10}H_{15}NO$	[M + H]+	166.3
4	1.22	Pseudoephedrine	$C_{10}H_{15}NO$	[M + H]+	166.3
5	3.43	Liquiritin	C21H22O9	[M + H]+	419.1
6	3.43	Liquiritin apiosid	C26H30O13	[M + H]+	551.1
7	4.17	Ononin	C22H22O9	[M + H]+	431.1
8	5.34	Glycyrrhizic acid	C42H62O16	[M + H]+	823.4
9	5.34	Glycyrrhetinic acid	C30H46O4	[M + H]+	471.3

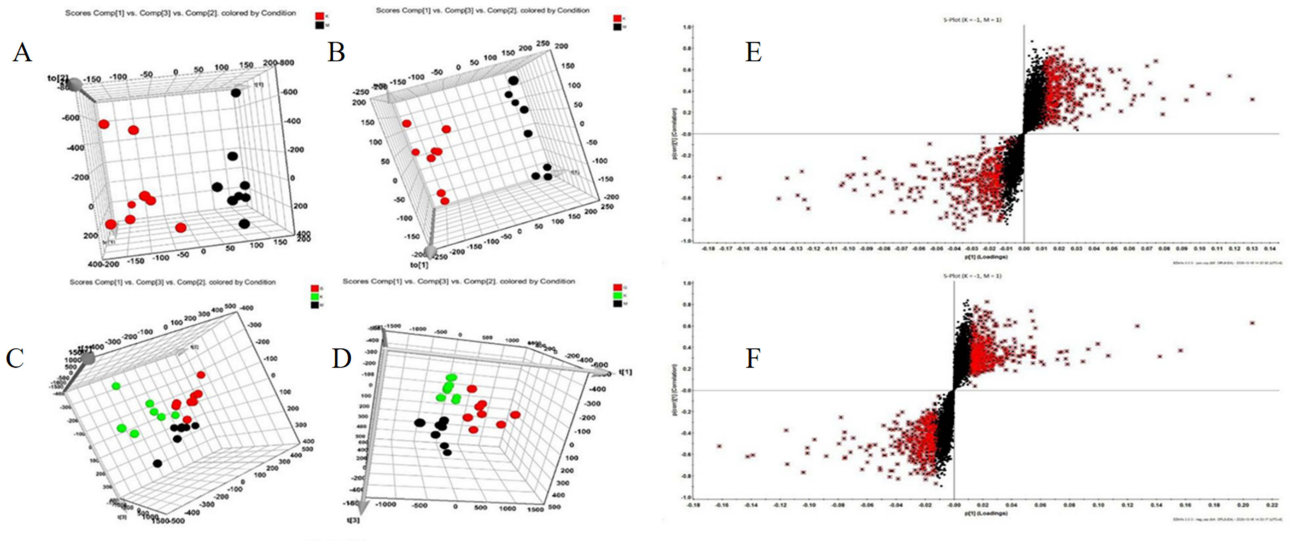

Figure 3 PCA score plots of plasma samples collected from the control group, the model group and treatment group. (**A**) PCA score plots for control and model group in positive mode; (**B**) PCA score plots for control and model group in negative mode; (**C**) PCA score plots of plasma samples collected from the control, the model group and the MXSGT group in positive mode; (**D**) PCA score plots of plasma samples collected from the control, the model group and the MXSGT group in negative mode; (**E**) S-plot score in positive mode; (**F**) S-plot score in negative mode.

The results showed that compared with the control group, the abundance of asthma-related chemicals in the model group changed significantly ($p < 0.05$). These chemical abundances were reversed in the MXSGT group, suggesting they may be potential biomarkers. Twelve biomarkers showed reversal after MXSGT administration (Figure 4).

These potential biomarkers accurately represent OVA-induced allergic asthma metabolism. Through exploration of relevant metabolic pathways, we established a metabolic network for potential biomarkers and pathways based on comprehensive network analysis. These include TCA cycle, alanine, aspartate and glutamate metabolism, tyrosine metabolism, etc. Pathway involvement suggests a potential mechanism for MXSGT's effects. TCA cycle emerged as the major metabolic pathway, involving three biomarkers: oxoglutaric acid, isocitric acid, and succinic acid (Figure 5).

Metabolite Identification

According to the protocol described above, 12 potential biomarkers were tentatively identified and characterized, and they were summarized in Tables 2 and 3.

As seen in Figure 6, a clustering heat map showed differences in relative values among the control, model, and treatment groups. The 12 asthma-related biomarkers identified through metabolomics technology exhibited varying degrees of recovery following MXSGT treatment.

The biomarkers were imported into the Metscape plugin in Cytoscape to further understand their correlations. We constructed a metabolite–reaction interaction network based on metabolic pathways (Figure 7). The results revealed that succinate, 2-oxoglutarate, and L-noradrenaline are associated with the TCA cycle. Succinate and 2-oxoglutarate are also linked to the urea cycle and metabolism of arginine, proline, glutamate, aspartate, and asparagine. Furthermore, succinate participates in phytanic acid peroxisomal oxidation and butanoate metabolism. Therefore, we conclude that succinate is the most significant biomarker in both asthma pathogenesis and MXSGT treatment.

Network Pharmacology Research

Prediction of Active Ingredients and Disease Targets

By searching the TCMSP, SwissADME, and SwissTargetPrediction databases, a total of 102 active ingredients were selected to predict targets. This selection included 76 from licorice, 16 from ephedra, and 10 from almond. Gypsum was not recorded because it was not found in TCMSP. From this selection, 749 common active ingredient targets were identified, which included 132 overlapping targets (Figure 8A). To identify disease targets, searches were conducted

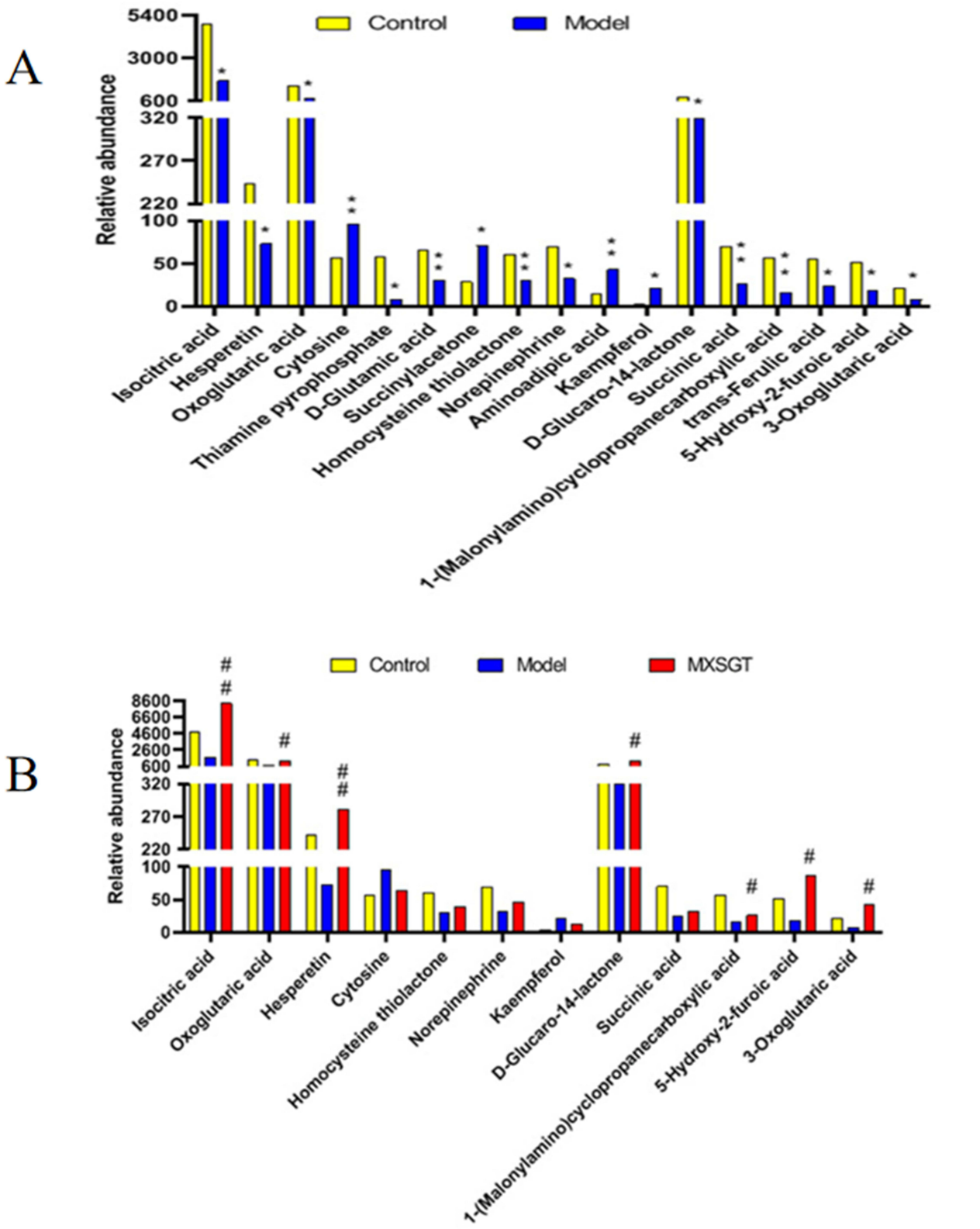

Figure 4 Changes in the peak area levels (mean) of target metabolites, (**A**) control group compared with model group (*p<0.05, **p<0.01); (**B**) comparison of MXSGT group and model group(#p<0.05, ##p<0.01).

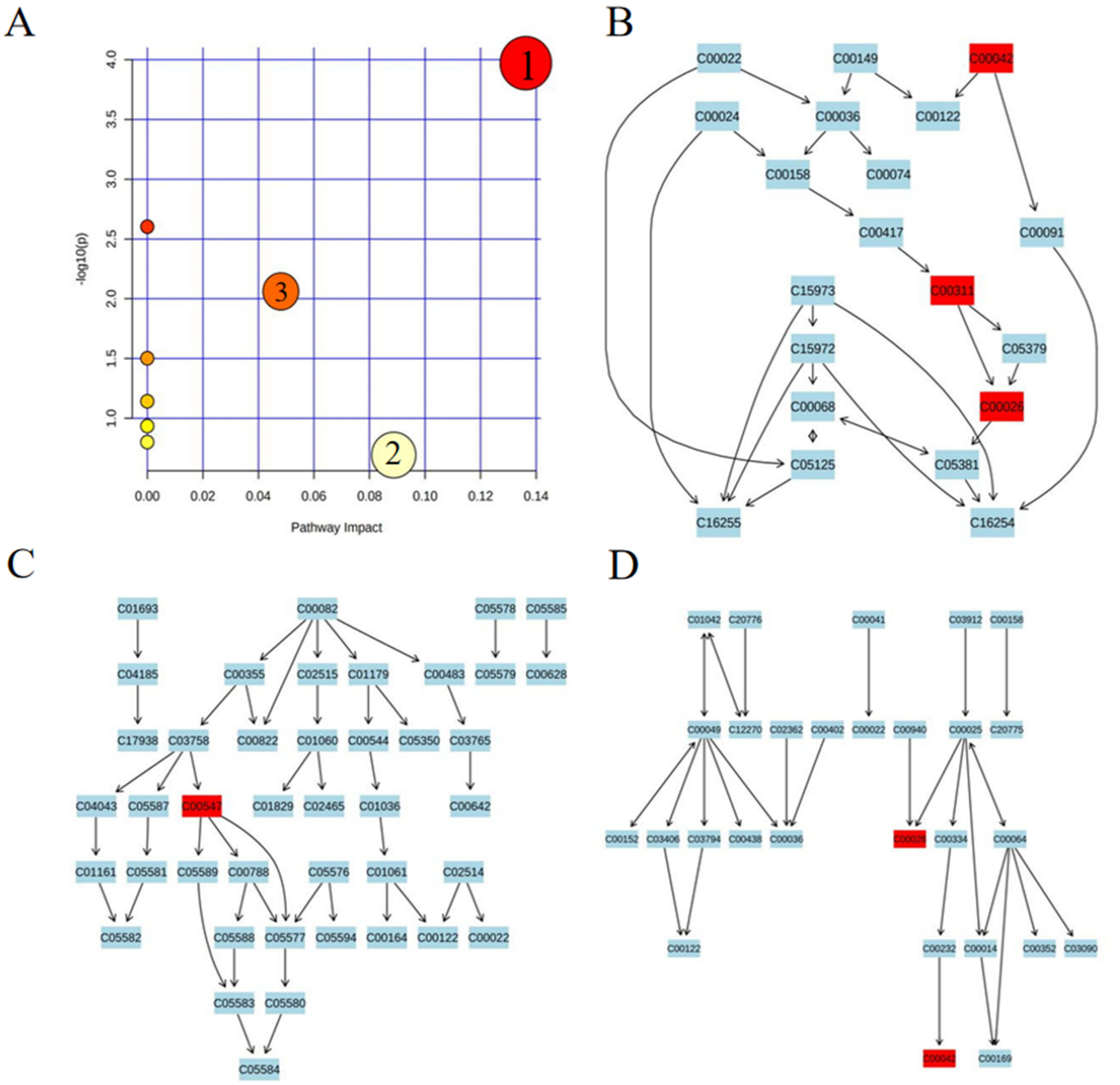

Figure 5 Summary of pathway analysis with MetPA. (**A**) 1. The Citrate cycle (TCA cycle); 2. Tyrosine metabolism; 3. Alanine, aspartate and glutamate metabolism. (**B**) TCA cycle; (**C**) Tyrosine metabolism; (**D**) Alanine, aspartate and glutamate metabolism.

using the keyword "asthma" in the GeneCards and OMIM databases. After merging and deduplicating the results, a total of 1167 disease targets were obtained. The active ingredient targets and disease targets were subsequently analyzed using Venny 2.1.0, resulting in the identification of 181 intersection targets (Figure 8B). These intersection targets represent potential therapeutic targets for MXSGT in asthma treatment.

Protein–Protein Interaction (PPI) Network Analysis

Importing the 181 intersection targets into the STRING database for protein interaction analysis. Using Cytoscape 3.10.2, a PPI network diagram was generated after data export. Nodes with darker colors and larger volumes represent higher interaction scores and tighter protein–protein interactions. Observing Figure 9A, TNF exhibits the darkest color and

https://doi.org/10.2147/JIR.S515631

Table 2 Potential Biomarkers Identified in Positive Ion Mode

No.	m/z	Tr (min)	Chemical Formula	Metabolites	HMDB Code	VIP	Model/ Control	MXSGT/ Model
1	1.18_ 192.0268	1.18	$C_6H_8O_7$	D-Glucaro-1,4-lactone	HMDB 41862	7.7214	↓	↑
2	1.59_ 101.0236	1.59	$C_4H_6O_4$	Succinate	HMDB 00254	2.8220	↓	↑
3	1.67_ 187.0478	1.67	$C_7H_9NO_5$	1-(Malonylamino) cyclopropanecarboxylic acid	HMDB 31700	2.7843	↓	↑
4	1.17_ 128.0110	1.17	$C_5H_4O_4$	5-Hydroxy-2-furoic acid	HMDB 59784	1.9612	↓	↑
5	1.18_ 147.0285	1.18	$C_5H_6O_5$	3-Oxoglutaric acid	HMDB 13701	1.1850	↓	↑

Table 3 Potential Biomarkers Identified in Negative Ion Mode

No.	m/z	Tr (min)	Chemical Formula	Metabolites	HMDB Code	VIP	Model/ Control	MXSGT/ Model
1	1.16_ 192.0278	1.16	$C_6H_8O_7$	Isocitrate	HMDB 00193	13.1588	↓	↑
2	0.89_ 145.0155	0.89	$C_5H_6O_5$	2-Oxoglutarate	HMDB 00208	6.4784	↓	↑
3	4.54_ 283.0612	4.54	$C_{16}H_{14}O_6$	Hesperetin	HMDB 05782	3.0808	↓	↑
4	4.30_ 221.079	4.30	$C_4H_5N_3O$	Cytosine	HMDB 00630	1.7753	↑	↓
5	3.69_ 233.0435	3.69	C_4H_7NOS	Homocysteine thiolactone	HMDB 02287	1.4925	↓	↑
6	3.26_ 150.0571	3.26	$C_8H_{11}NO_3$	L-noradrenaline	HMDB 00216	1.4849	↓	↑
7	0.91_ 285.0403	0.91	$C_{15}H_{10}O_6$	Kaempferol	HMDB 05801	1.0091	↑	↓

largest size, indicating its role as a key therapeutic target for MXSGT in asthma treatment. We identified the top 15 hub targets to establish the core target PPI network (Figure 9B).

Gene Ontology (GO) Enrichment Analysis and KEGG Pathway Analysis

We imported the intersection targets of MXSGT and asthma into ADVID for GO enrichment and KEGG pathway analysis, resulting in a total of 104 GO entries ($p < 0.01$). Among these, 71 entries were associated with biological processes (BPs), primarily focusing on positive regulation of DNA-templated transcription, positive regulation of transcription by RNA polymerase II, and negative regulation of gene expression (Figure 10A). There were 11 entries related to cellular components (CCs), mainly including cytoplasm, nuclear regulation, and nucleoplasm (Figure 10B). Additionally, 22 entries pertained to molecular functions (MFs), with a focus on protein binding, identical protein binding, and enzyme binding (Figure 10C). A bubble plot illustrating the top 10 GO categories in each of the three domains is shown in Figure 10D. Through KEGG pathway enrichment analysis ($p < 0.01$), we identified a total of 64

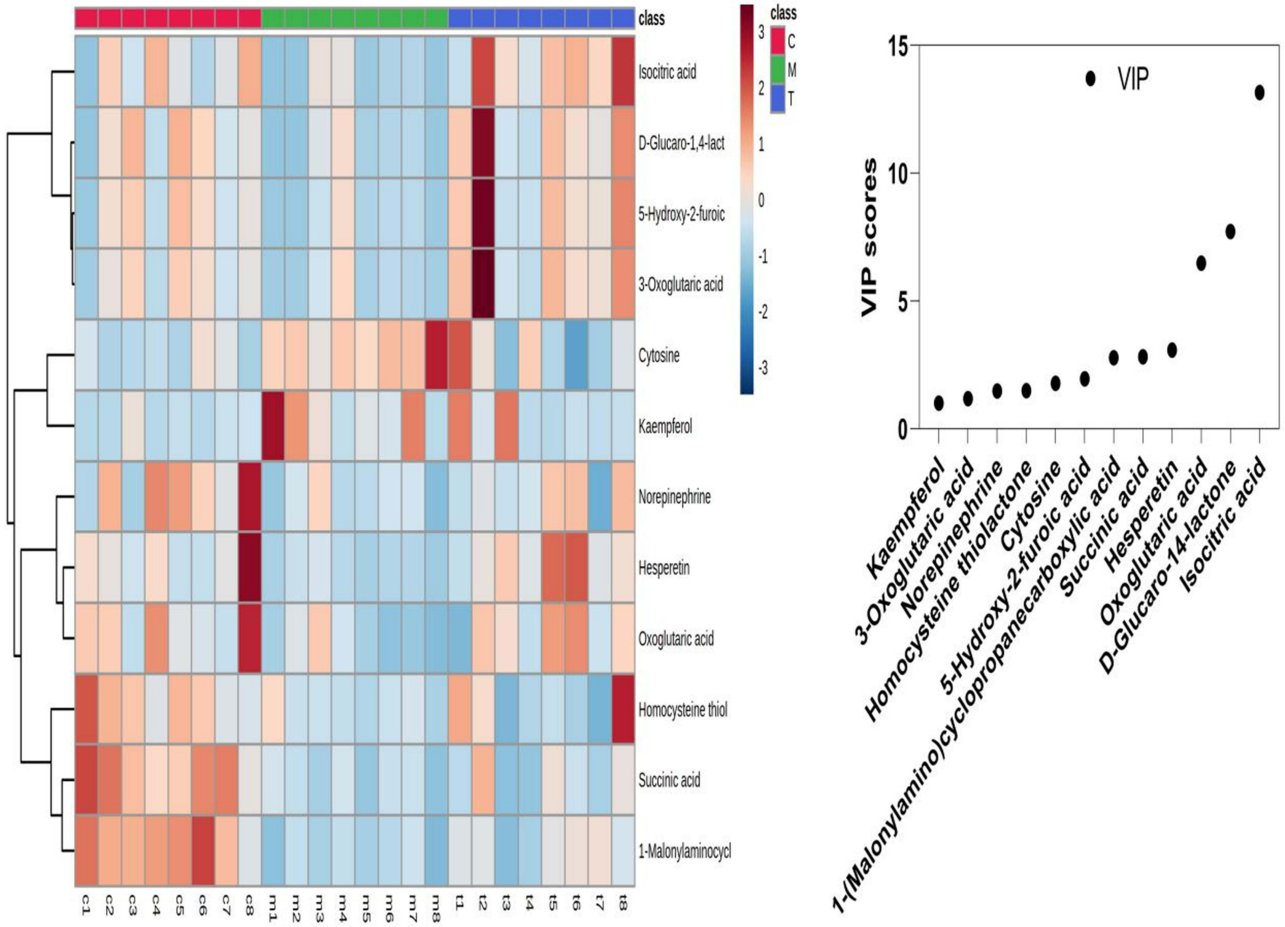

Figure 6 Heatmap visualisation for serum samples from the control, model, and treatment group.

relevant pathways, including those related to cancer, Hepatitis B, proteoglycans in cancer, and lipid metabolism and atherosclerosis. The top 15 pathways were selected according to ascending p-value order. Subsequently, a bar chart illustrated these findings (Figure 10E).

Target-Based Pathway Analysis

In order to further investigate the relationship between targets and metabolic pathways, we input the top target (TNF) and three proteins (NF-κBp65, p38-MAPK, and TGF-β1) into KEGG. The results showed that TNF was involved in the MAPK signaling pathway and NF-κB signaling pathway (Figure 11), which are upstream of NF-κBp65 and p38-MAPK. Therefore, the expression of NF-κBp65 and p38-MAPK are closely associated with TNF.

Molecular Docking

Two blood compounds (pseudoephedrine and glycyrrhetinic acid) were screened as MXSGT core components, and molecular docking was performed with TNF. Typically, a binding energy of less than −5 kcal/mol indicates a stable interaction between the ligand and the target protein,[20] with lower binding energies correlating to increased stability of the interaction. In the present study, molecular docking results indicated that both pseudoephedrine and glycyrrhetinic acid have high affinity to TNF via hydrogen bonds (Figure 12), with binding energies of −5.44 and −8.79 kcal/mol, respectively, suggesting a strong ligand-receptor affinity.[21]

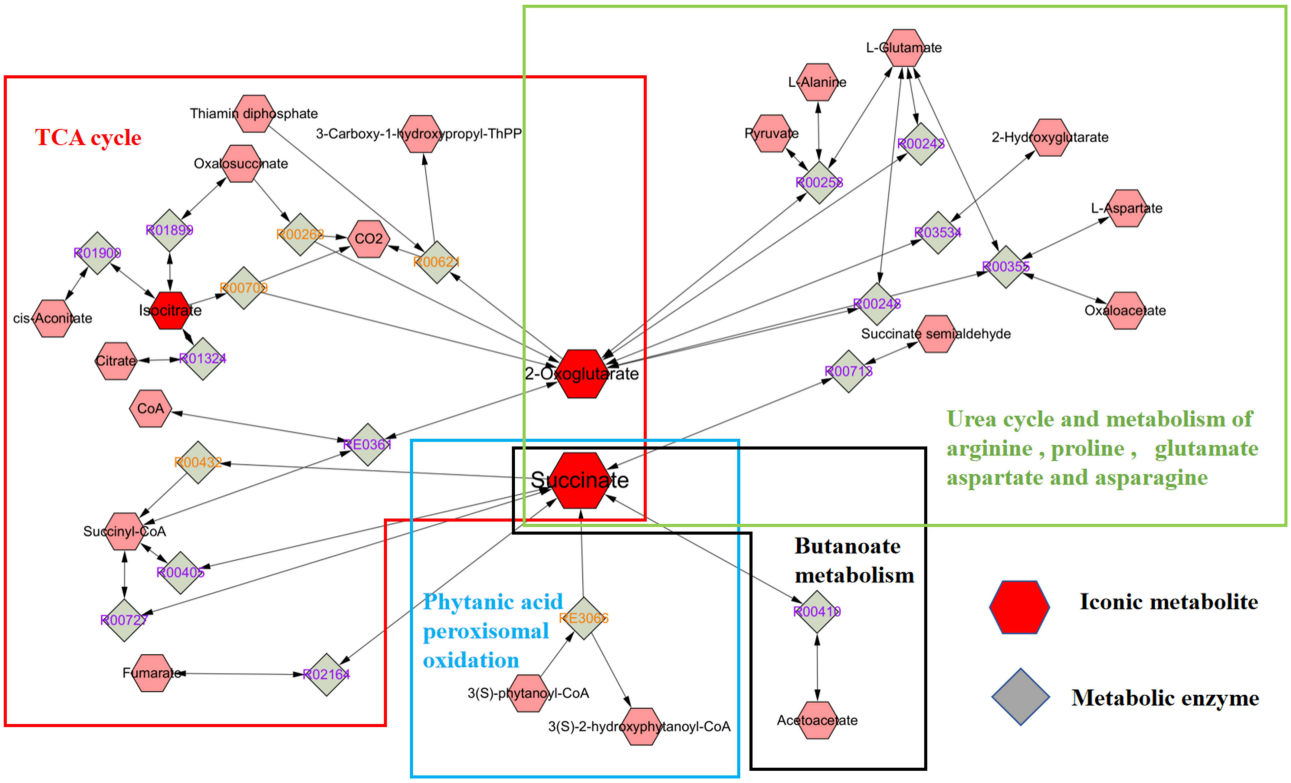

Figure 7 The metabolite–reaction interaction network of biomarkers.

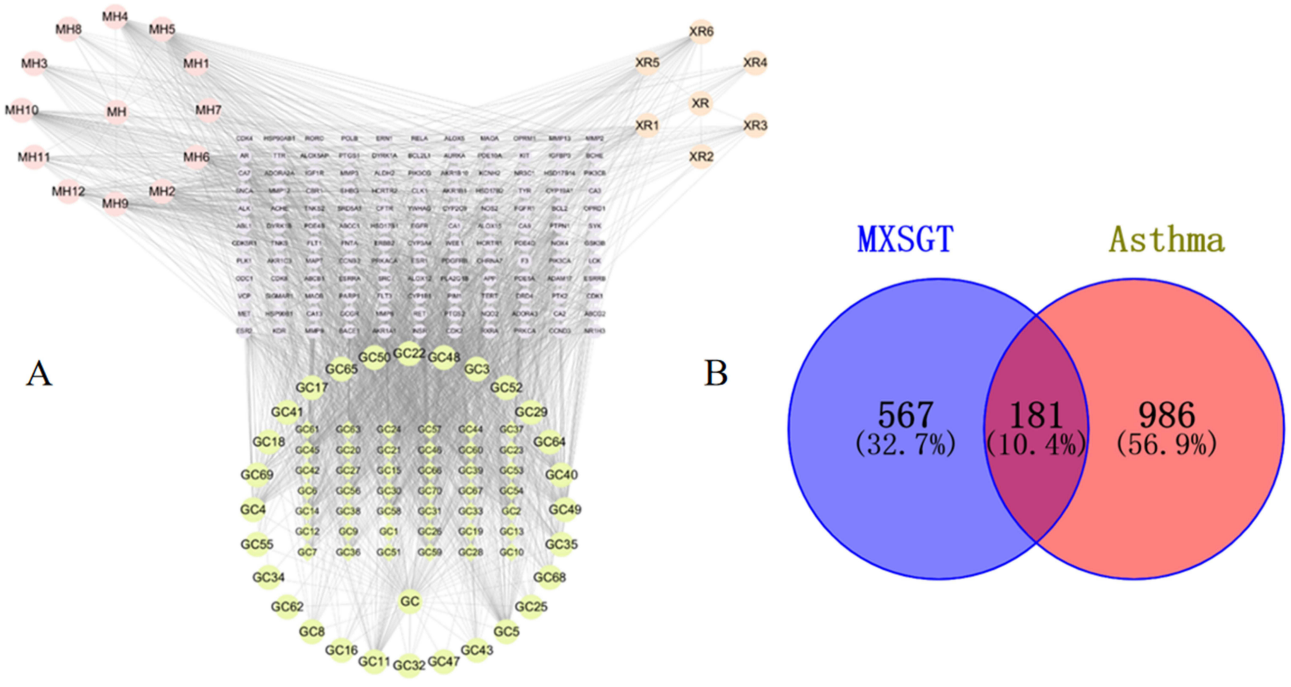

Figure 8 Prediction of active ingredients and disease targets. (**A**) Common active ingredient targets' interaction network, (**B**) Venn diagram.

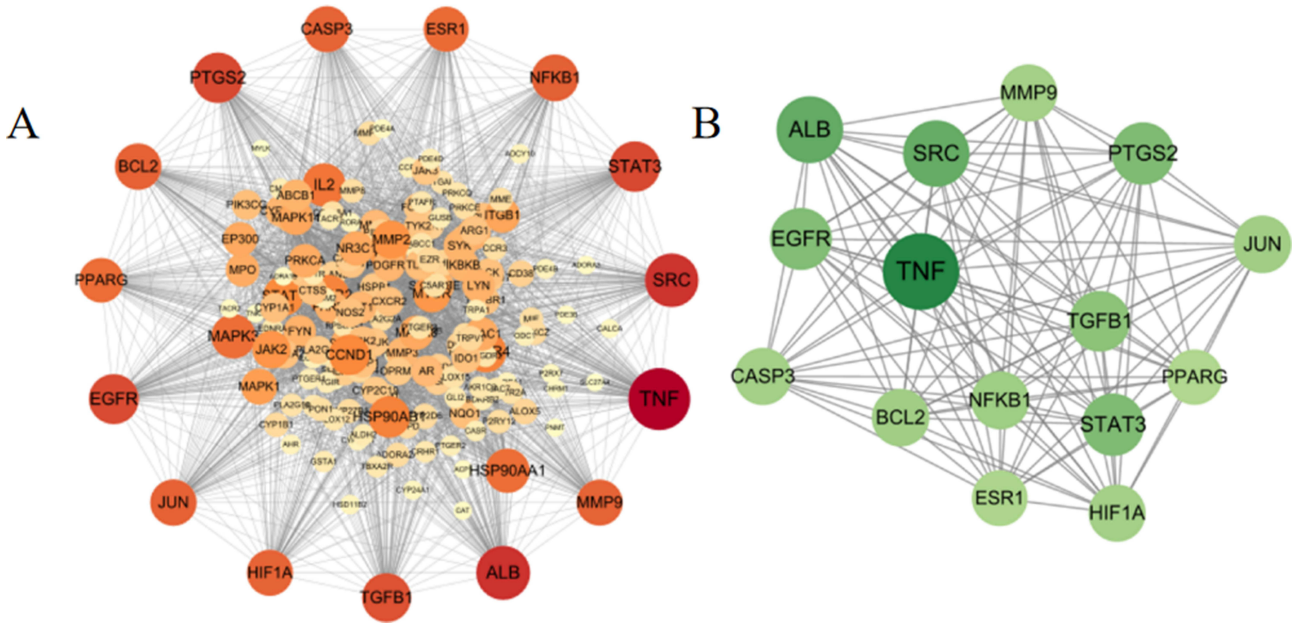

Figure 9 PPI network analysis. (**A**) PPI network diagram of interacting targets, (**B**) hub targets.

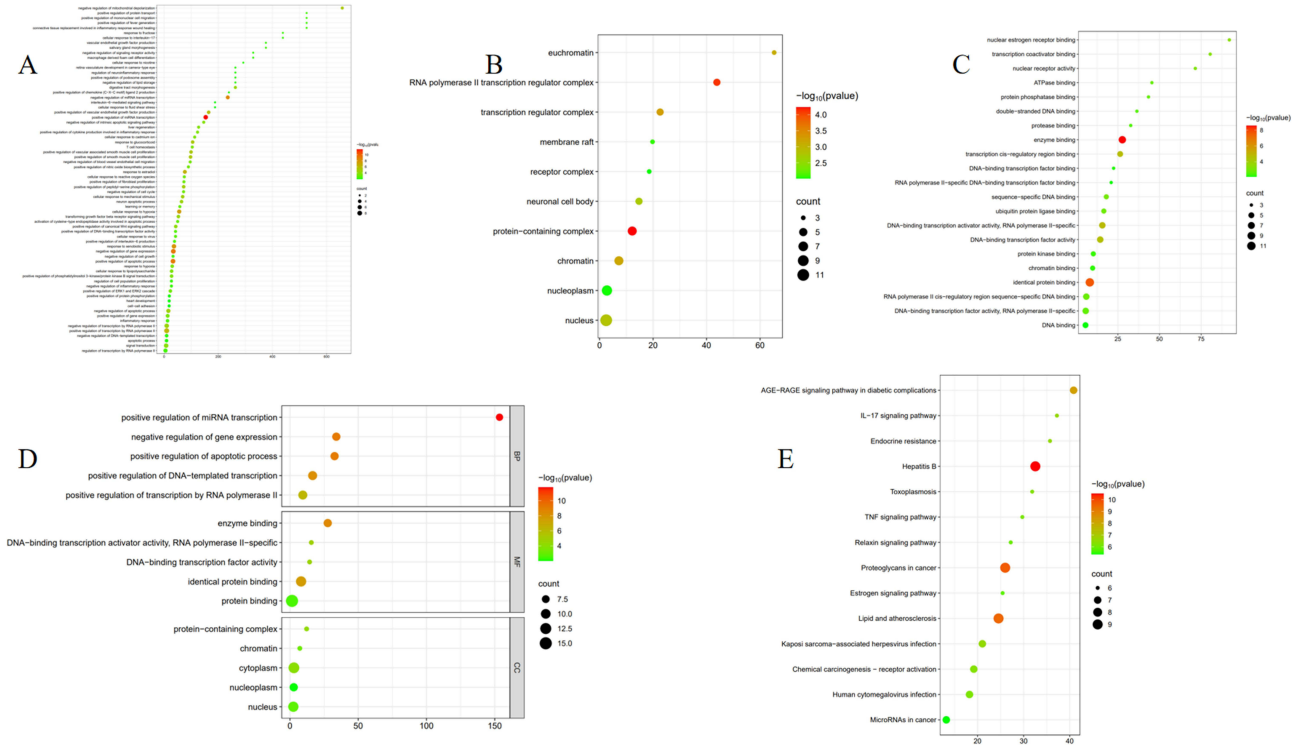

Figure 10 GO enrichment analysis and KEGG pathway analysis. (**A**) GO BP enrichment analysis, (**B**) GO CC enrichment analysis, (**C**) GO MF enrichment analysis, (**D**) the top 5 GO enrichment analysis in each domains, (**E**) KEGG enrichment analysis.

Discussion

Metabolomics combined with network pharmacology has become one of the important methods for studying the mechanisms of TCM in treating diseases.[22] Metabolomics research identifies potential metabolites and related pathways,

https://doi.org/10.2147/JIR.S515631

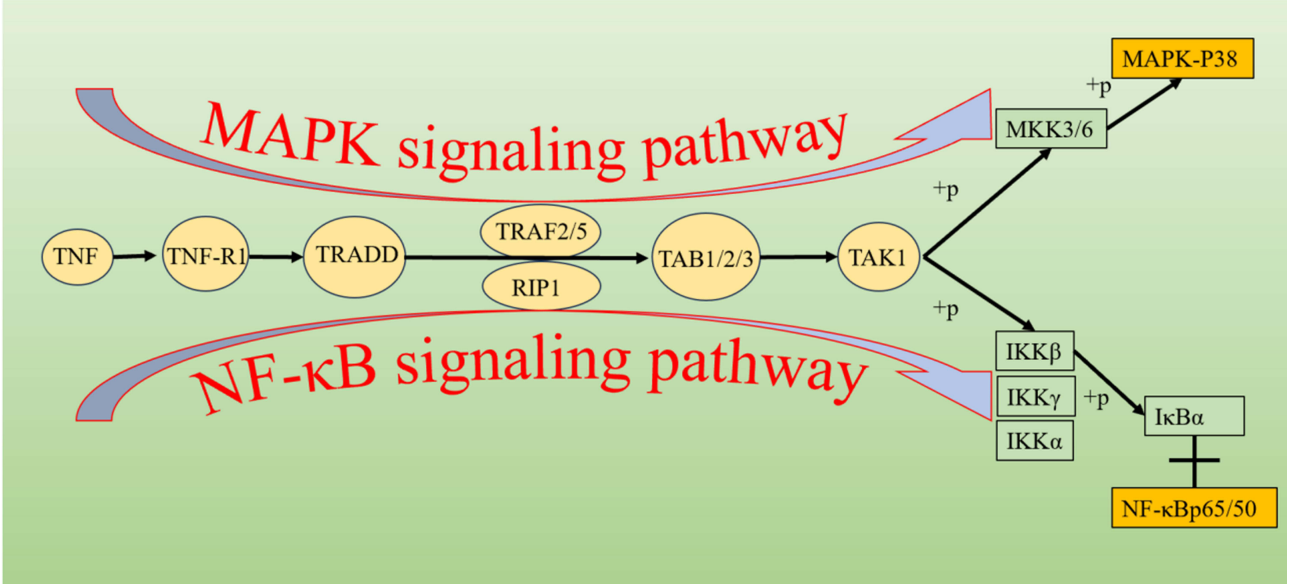

Figure 11 The MAPK and NF-κB pathways that link TNF, NFκBp65, and p38-MAPK.

while network pharmacology predicts interactions between TCM components and proteins. Based on this, we comprehensively and deeply explain the therapeutic effects of TCM.

In metabolomics analysis, 12 distinct metabolites were identified between the MXSGT-treated and model groups. Pathway analysis indicated that MXSGT's effectiveness involved multiple factors, including impacts on protein synthesis, vascular protection, and immune homeostasis, highlighting the multi-target nature of TCM. Specifically, MXSGT significantly increased levels of succinate, D-glucaro-1,4-lactone, 1-(malonylamino) cyclopropanecarboxylic acid, 5-hydroxy-2-furoic acid, 3-oxoglutaric acid, isocitrate, 2-oxoglutarate, hesperetin, homocysteine thiolactone, and L-noradrenaline, while decreasing cytosine and kaempferol. Succinate, an intermediate in TCA cycle, is significantly altered in asthma patients.[23] SUCNR1, a sensor for extracellular succinic acid, plays an important role in mediating inflammatory processes. Experimental reports show SUCNR1 is highly expressed on mast cells and upregulated by IL-4. Succinate binding to SUCNR1 induces mast cell degranulation, releasing cytokines (IL-5, IL-6, IL-1β, IL-17A) and inflammatory mediators (leukotrienes, prostaglandins, thromboxane).[24] As Gal et al noted, mast cells drive early-phase allergic airway inflammation, characterized by rapid airway smooth muscle contraction, tissue swelling, and increased mucus secretion.[25] Consequently, succinate is considered an important asthma biomarker. 2-Oxoglutarate, a key Krebs cycle intermediate, was upregulated by MXSGT. Notably, 2-oxoglutarate supplementation and elevated IDH2 levels alleviate severe lung diseases.[26,27] Chan Seo et al identified 2-oxoglutarate as a potential asthma biomarker.[28] L-Noradrenaline, a component of tyrosine metabolism, is demethylated by phenylethanolamine N-methyltransferase to form epinephrine. Epinephrine acts as a β2-adrenergic receptor agonist, relieving bronchospasm, dilating bronchi, improving ventilatory function, and inhibiting allergic mediator release – producing antiasthmatic effects via bronchial smooth muscle β2-receptor stimulation.[29] Hesperetin was upregulated by MXSGT. Hesperidin (hesperetin's glycoside precursor) inhibits dendritic cells (DCs).[30] DCs are professional antigen-presenting cells that stimulate naïve T cells and initiate CD4+ T cell differentiation into Th1/Th2 subsets.[31] Bronchial epithelial DCs activate CD4+ T cells and preferentially secrete Th2 cytokines (IL-4, IL-5),[32] promoting eosinophilic airway inflammation, hyperresponsiveness, and remodeling.[33] By increasing hesperetin, MXSGT may inhibit DCs, suppressing CD4+ T cell differentiation into Th2 subsets, reducing Th2 cytokine synthesis/release, and alleviating Th2-mediated eosinophilic airway inflammation.

Besides, we identified 9 blood components of MXSGT in serum samples from treated rats using UPLC-MS analysis. These included pseudoephedrine and glycyrrhetinic acid. Blood components are generally considered crucial bioactive mediators of TCM effects.[34] The anti-inflammatory properties of these ingredients have been confirmed in previous studies. Pseudoephedrine has demonstrated efficacy in treating asthma,[35] potentially linked to its ability to inhibit NF-κB/

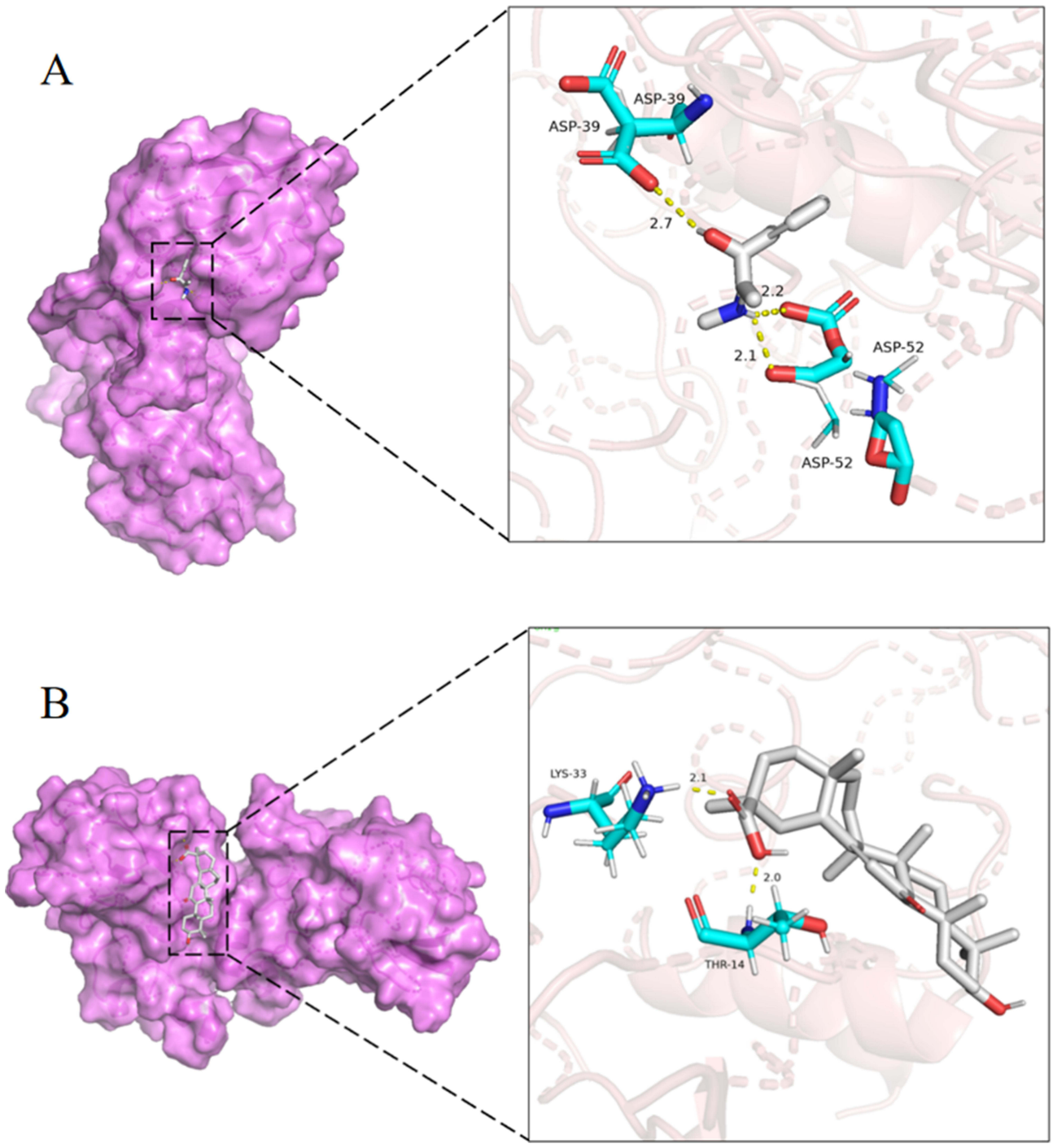

Figure 12 Visualization of molecular docking results. (**A**)TNF- pseudoephedrine, (**B**)TNF- glycyrrhetinic acid.

p65 nuclear translocation and reduce TNF production.[36] Similarly, Zhang and Liu et al experimentally demonstrated that glycyrrhetinic acid ameliorates bronchial smooth muscle inflammation by inhibiting the NF-κB signaling pathway and reducing inflammatory factors such as TNF-α, IL-4, and IL-6.[12,37] It is worth noting that these research results are consistent with our experimental results.

By combining metabolomics and network pharmacology, we gained a more precise and systematic understanding of MXSGT's anti-asthma network. We identified 3 key metabolites (succinate, isocitrate, and 2-oxoglutarate) and 4 related pathways (TCA cycle, phytanic acid peroxisomal oxidation, butanoate metabolism, and urea cycle/metabolism of arginine,

https://doi.org/10.2147/JIR.S515631

proline, glutamate, aspartate, and asparagine). Comprehensive analysis revealed that MAPK and NF-κB signaling pathways play key roles in asthma treatment. The NF-κB and MAPK signaling pathways are prototypical pro-inflammatory pathways and contribute significantly to asthma pathogenesis.[38,39] NF-κB activation is essential for IL-1β-induced HIF1A upregulation via the canonical NF-κB pathway, enabling IL-1β to upregulate Muc5ac expression in asthma.[40] Airway smooth muscle cells (ASMCs) are vital in asthma pathogenesis. IL-37 significantly upregulates IκB expression while downregulating NF-κB p65 levels and phosphorylation in both OVA-induced mice and TGF-β1-stimulated ASMCs; furthermore, it markedly suppresses TGF-β1-induced ASMC proliferation, migration, epithelial–mesenchymal transition, and inflammatory responses, thereby alleviating airway inflammation and remodeling in asthma.[41]

In our study, molecular docking and immunohistochemistry experiments validated MXSGT's interaction with the MAPK and NF-κB signaling pathways. These results indicate that MXSGT components (eg, pseudoephedrine and glycyrrhetinic acid) tightly bind to TNF and reduce NF-κB p65, p38-MAPK, and TGF-β1 expression. The TNF-asthma association primarily stems from TNF's pivotal signaling role. Studies show TNF regulates HIF1A protein/mRNA expression via NF-κB-dependent pathways, affecting ASMC function and airway inflammatory disease development.[42] Furthermore, KEGG-based drug classification implicates TNF in NF-κB and MAPK signaling pathways.[43–46] Among MAPK family members, p38-MAPK is most prominently involved in asthma-related airway/lung inflammation.[47] p38-MAPK induces Th2 cell differentiation/activation, promotes IL-4, IL-5, and IL-13 release, increases airway eosinophils, and contributes to IgE production, eosinophilic inflammation, and bronchial hyperresponsiveness.[47–49] p38-MAPK also significantly contributes to T2-low neutrophilic airway inflammation by upregulating ICAM-1 on lung vascular endothelial cells and increasing IL-6, IL-8, and MCP-1 secretion, thereby inhibiting neutrophil apoptosis.[50] Research indicates p38-MAPK involvement in airway remodeling; for example, lung fibroblasts proliferate and secrete collagen upon mast cell contact via p38-MAPK-mediated IL-6 release.[51] These results suggest MXSGT alleviates inflammation by inhibiting MAPK and NF-κB signaling pathways.

Despite the prospective findings, this study had several limitations. We discovered some potential molecular mechanisms of MXSGT in treating asthma, but as a whole, the mechanism of MXSGT as a TCM formula for treating asthma is complex and extensive, and we still lack further in-depth research. Furthermore, our study is limited to OVA-induced asthma rats, and the therapeutic effect of MXSGT on other intrinsic types such as TH2-reduced asthma is not yet clear. Therefore, future research can focus on these aspects, which will help us better understand the mechanism of MXSGT in the treatment of asthma.

Conclusions

In summary, this study integrated network pharmacology and metabolomics to investigate the molecular mechanism of MXSGT in treating asthma. Our study demonstrated that MXSGT achieves anti-inflammatory and anti-asthma effects by targeting TNF and inhibiting inflammatory mediator release through the MAPK signaling pathway and NF-κB pathways. Integration of metabolomics and network pharmacology provides valuable insights into research on molecular mechanisms of TCM in treating diseases.

Data Sharing Statement

The data generated in this study are available from the corresponding author on reasonable request.

Author Contributions

All authors made significant contribution to the work reported, whether that is in the conception, study design, execution, acquisition of data, analysis and interpretation, or in all these areas; took part in drafting, revising or critically reviewing the article; gave final approval of the version to be published; have agreed on the journal to which the article has been submitted; and agree to be accountable for all aspects of the work.

Funding

National Natural Science Foundation of China (Grant No. 81973746); Doctoral research start-up fund of Lishui University (Grant No. QD 2421); New Seed Project of Lishui University, Zhejiang Province (Grant No. 2024R433A005); School enterprise cooperation course project between Traditional Chinese Medicine Hospital

and Health Industry College (Grant No. 23CYKC07); National College Students Innovation and Entrepreneurship Training Program (Grant No. S202410352042); 2025 Zhejiang Provincial Administration of Traditional Chinese Medicine Project (Grant No. 2025ZL626).

Disclosure

The authors report no conflicts of interest in this work.

References

1. Oh J, Kim S, Kim MS. Global, regional, and national burden of asthma and atopic dermatitis, 1990-2021, and projections to 2050: a systematic analysis of the global burden of disease study 2021. *Lancet Respir Med*. 2025;13(5):425–446. doi:10.1016/s2213-2600(25)00003-7
2. Lötvall J, Akdis CA, Bacharier LB, et al. Asthma endotypes: a new approach to classification of disease entities within the asthma syndrome. *J Allergy Clin Immunol*. 2011;127(2):355–360. doi:10.1016/j.jaci.2010.11.037
3. Sharma S, Gerber AN, Kraft M, Wenzel SE. Asthma pathogenesis: phenotypes, therapies, and gaps: summary of the aspen lung conference 2023. *Am J Respir Cell Mol Biol*. 2024;71(2):154–168. doi:10.1165/rcmb.2024-0082WS
4. Fahy JV. Type 2 inflammation in asthma--present in most, absent in many. *Nat Rev Immunol*. 2015;15(1):57–65. doi:10.1038/nri3786
5. Lee MY, Seo CS, Lee NH, et al. Anti-asthmatic effect of schizandrin on OVA-induced airway inflammation in a murine asthma model. *Int Immunopharmacol*. 2010;10(11):1374–1379. doi:10.1016/j.intimp.2010.07.014
6. Wenzel SE. Asthma phenotypes: the evolution from clinical to molecular approaches. *Nat Med*. 2012;18(5):716–725. doi:10.1038/nm.2678
7. Guo T, Guo Y, Liu Q, et al. The TCM prescription Ma-xing-shi-gan-tang inhibits Streptococcus pneumoniae pathogenesis by targeting pneumolysin. *J Ethnopharmacol*. 2021;275:114133. doi:10.1016/j.jep.2021.114133
8. Hsieh CF, Lo CW, Liu CH, et al. Mechanism by which Ma-xing-shi-gan-tang inhibits the entry of influenza virus. *J Ethnopharmacol*. 2012;143(1):57–67. doi:10.1016/j.jep.2012.05.061
9. Pi W, Han N, Wu L, et al. Discovery, traceability, formation mechanism, metal and organic components analysis of supramolecules from Maxing Shigan decoction. *J Pharm Biomed Anal*. 2023;234:115532. doi:10.1016/j.jpba.2023.115532
10. Huang XF, Cheng WB, Jiang Y, et al. A network pharmacology-based strategy for predicting anti-inflammatory targets of ephedra in treating asthma. *Int Immunopharmacol*. 2020;83:106423. doi:10.1016/j.intimp.2020.106423
11. Cui W, Zhou H, Liu YZ, et al. Amygdalin improves allergic asthma via the thymic stromal lymphopoietin-dendritic cell-OX40 ligand axis in a mouse model. *Iran J Allergy Asthma Immunol*. 2023;22(5):430–439. doi:10.18502/ijaai.v22i5.13993
12. Liu J, Xu Y, Yan M, Yu Y, Guo Y. 18β-Glycyrrhetinic acid suppresses allergic airway inflammation through NF-κB and Nrf2/HO-1 signaling pathways in asthma mice. *Sci Rep*. 2022;12(1):3121. doi:10.1038/s41598-022-06455-6
13. Nicholson JK, Lindon JC. Systems biology: metabonomics. *Nature*. 2008;455(7216):1054–1056. doi:10.1038/4551054a
14. Fang H, Zhang A, Yu J, et al. Insight into the metabolic mechanism of scoparone on biomarkers for inhibiting Yanghuang syndrome. *Sci Rep*. 2016;6:37519. doi:10.1038/srep37519
15. Liu Q, Zhang A, Wang L, et al. High-throughput chinmedomics-based prediction of effective components and targets from herbal medicine AS1350. *Sci Rep*. 2016;6:38437. doi:10.1038/srep38437
16. Niu B, Xie X, Xiong X, Jiang J. Network pharmacology-based analysis of the anti-hyperglycemic active ingredients of roselle and experimental validation. *Comput Biol Med*. 2022;141:104636. doi:10.1016/j.compbiomed.2021.104636
17. Zhao Y, Li H, Li X, et al. Network pharmacology-based analysis and experimental in vitro validation on the mechanism of Paeonia lactiflora Pall. in the treatment for type I allergy. *BMC Complement Med Ther*. 2022;22(1):199. doi:10.1186/s12906-022-03677-z
18. Bauermeister A, Mannochio-Russo H, Costa-Lotufo LV, Jarmusch AK, Dorrestein PC. Mass spectrometry-based metabolomics in microbiome investigations. *Nat Rev Microbiol*. 2022;20(3):143–160. doi:10.1038/s41579-021-00621-9
19. Jiashuo WU, Fangqing Z, Zhuangzhuang LI, Weiyi J, Yue S. Integration strategy of network pharmacology in Traditional Chinese Medicine: a narrative review. *J Tradit Chin Med*. 2022;42(3):479–486. doi:10.19852/j.cnki.jtcm.20220408.003
20. Liao F, Yousif M, Huang R, Qiao Y, Hu Y. Network pharmacology- and molecular docking-based analyses of the antihypertensive mechanism of Ilex kudingcha. *Front Endocrinol*. 2023;14:1216086. doi:10.3389/fendo.2023.1216086
21. Pinzi L, Rastelli G. Molecular docking: shifting paradigms in drug discovery. *Int J Mol Sci*. 2019;20(18):4331. doi:10.3390/ijms20184331
22. Du H, Shao M, Xu S, et al. Integrating metabolomics and network pharmacology analysis to explore mechanism of Pueraria lobata against pulmonary fibrosis: involvement of arginine metabolism pathway. *J Ethnopharmacol*. 2024;332:118346. doi:10.1016/j.jep.2024.118346
23. Chang C, Guo ZG, He B, Yao WZ. Metabolic alterations in the sera of Chinese patients with mild persistent asthma: a GC-MS-based metabolomics analysis. *Acta Pharmacol Sin*. 2015;36(11):1356–1366. doi:10.1038/aps.2015.102
24. Tang X, Rönnberg E, Säfholm J, et al. Activation of succinate receptor 1 boosts human mast cell reactivity and allergic bronchoconstriction. *Allergy*. 2022;77(9):2677–2687. doi:10.1111/all.15245
25. Galli SJ, Tsai M, Piliponsky AM. The development of allergic inflammation. *Nature*. 2008;454(7203):445–454. doi:10.1038/nature07204
26. Yeung BHY, Huang J, An SS, Solway J, Mitzner W, Tang WY. Role of isocitrate dehydrogenase 2 on DNA hydroxymethylation in human airway smooth muscle cells. *Am J Respir Cell Mol Biol*. 2020;63(1):36–45. doi:10.1165/rcmb.2019-0323OC
27. Vohwinkel CU, Lecuona E, Sun H, et al. Elevated CO(2) levels cause mitochondrial dysfunction and impair cell proliferation. *J Biol Chem*. 2011;286(43):37067–37076. doi:10.1074/jbc.M111.290056
28. Seo C, Hwang YH, Lee HS, et al. Metabolomic study for monitoring of biomarkers in mouse plasma with asthma by gas chromatography-mass spectrometry. *J Chromatogr B Analyt Technol Biomed Life Sci*. 2017;1063:156–162. doi:10.1016/j.jchromb.2017.08.039
29. Abroug F, Dachraoui F, Ouanes-Besbes L. Our paper 20 years later: the unfulfilled promises of nebulised Adrenaline in acute severe asthma. *Intensive Care Med*. 2016;42(3):429–431. doi:10.1007/s00134-016-4210-1
30. Gu X, Zhou L, Du Q, et al. Hesperetin inhibits the maturation and function of monocyte-derived dendritic cells from patients with asthma. *Mol Med Rep*. 2009;2(3):509–513. doi:10.3892/mmr_00000129

31. Banchereau J, Steinman RM. Dendritic cells and the control of immunity. *Nature*. 1998;392(6673):245–252. doi:10.1038/32588
32. Vermaelen K, Pauwels R. Pulmonary dendritic cells. *Am J Respir Crit Care Med*. 2005;172(5):530–551. doi:10.1164/rccm.200410-1384SO
33. van Rijt LS, Jung S, Kleinjan A, et al. In vivo depletion of lung CD11c+ dendritic cells during allergen challenge abrogates the characteristic features of asthma. *J Exp Med*. 2005;201(6):981–991. doi:10.1084/jem.20042311
34. Ma FX, Xue PF, Wang YY, Wang YN, Xue SY. Research progress of serum pharmacochemistry of traditional Chinese medicine. *Zhongguo Zhong Yao Za Zhi*. 2017;42(7):1265–1270. doi:10.19540/j.cnki.cjcmm.20170224.010
35. Głowacka K, Wiela-Hojeńska A. Pseudoephedrine-Benefits and Risks. *Int J Mol Sci*. 2021;22(10):5146. doi:10.3390/ijms22105146
36. Wu Z, Kong X, Zhang T, Ye J, Fang Z, Yang X. Pseudoephedrine/ephedrine shows potent anti-inflammatory activity against TNF-α-mediated acute liver failure induced by lipopolysaccharide/D-galactosamine. *Eur J Pharmacol*. 2014;724:112–121. doi:10.1016/j.ejphar.2013.11.032
37. Zhang T, Liao JY, Yu L, Liu GS. Regulating effect of glycyrrhetinic acid on bronchial asthma smooth muscle proliferation and apoptosis as well as inflammatory factor expression through ERK1/2 signaling pathway. *Asian Pac J Trop Med*. 2017;10(12):1172–1176. doi:10.1016/j.apjtm.2017.10.025
38. Lawrence T. The nuclear factor NF-kappaB pathway in inflammation. *Cold Spring Harb Perspect Biol*. 2009;1(6):a001651. doi:10.1101/cshperspect.a001651
39. Yeung YT, Aziz F, Guerrero-Castilla A, Arguelles S. Signaling pathways in inflammation and anti-inflammatory therapies. *Curr Pharm Des*. 2018;24(14):1449–1484. doi:10.2174/1381612824666180327165604
40. Wu S, Li H, Yu L, Wang N, Li X, Chen W. IL-1β upregulates Muc5ac expression via NF-κB-induced HIF-1α in asthma. *Immunol Lett*. 2017;192:20–26. doi:10.1016/j.imlet.2017.10.006
41. Huang N, Liu K, Liu J, et al. Interleukin-37 alleviates airway inflammation and remodeling in asthma via inhibiting the activation of NF-κB and STAT3 signalings. *Int Immunopharmacol*. 2018;55:198–204. doi:10.1016/j.intimp.2017.12.010
42. Tsapournioti S, Mylonis I, Hatziefthimiou A, et al. TNFα induces expression of HIF-1α mRNA and protein but inhibits hypoxic stimulation of HIF-1 transcriptional activity in airway smooth muscle cells. *J Cell Physiol*. 2013;228(8):1745–1753. doi:10.1002/jcp.24331
43. Roy M, Singh K, Shinde A, et al. TNF-α-induced E3 ligase, TRIM15 inhibits TNF-α-regulated NF-κB pathway by promoting turnover of K63 linked ubiquitination of TAK1. *Cell Signal*. 2022;91:110210. doi:10.1016/j.cellsig.2021.110210
44. Chen M, Chen Z, Huang D, et al. Myricetin inhibits TNF-α-induced inflammation in A549 cells via the SIRT1/NF-κB pathway. *Pulm Pharmacol Ther*. 2020;65:102000. doi:10.1016/j.pupt.2021.102000
45. Zhang Y, Wang L, Bai L, Jiang R, Wu J, Li Y. Ebosin attenuates the inflammatory responses induced by TNF-α through inhibiting NF-κB and MAPK pathways in rat fibroblast-like synoviocytes. *J Immunol Res*. 2022;2022:9166370. doi:10.1155/2022/9166370
46. Guicciardi ME, Gores GJ. AIP1: a new player in TNF signaling. *J Clin Invest*. 2003;111(12):1813–1815. doi:10.1172/jci18911
47. Lambrecht BN, Hammad H, Fahy JV. The cytokines of asthma. *Immunity*. 2019;50(4):975–991. doi:10.1016/j.immuni.2019.03.018
48. Pelaia C, Vatrella A, Crimi C, Gallelli L, Terracciano R, Pelaia G. Clinical relevance of understanding mitogen-activated protein kinases involved in asthma. *Expert Rev Respir Med*. 2020;14(5):501–510. doi:10.1080/17476348.2020.1735365
49. Pelaia C, Paoletti G, Puggioni F, et al. Interleukin-5 in the Pathophysiology of Severe Asthma. *Front Physiol*. 2019;10:1514. doi:10.3389/fphys.2019.01514
50. Pelaia C, Vatrella A, Gallelli L, et al. Role of p38 mitogen-activated protein kinase in asthma and COPD: pathogenic aspects and potential targeted therapies. *Drug Des Devel Ther*. 2021;15:1275–1284. doi:10.2147/dddt.S300988
51. Fitzgerald SM, Lee SA, Hall HK, Chi DS, Krishnaswamy G. Human lung fibroblasts express interleukin-6 in response to signaling after mast cell contact. *Am J Respir Cell Mol Biol*. 2004;30(4):585–593. doi:10.1165/rcmb.2003-0282OC